Computer Modeling of the Active-Site Configurations within the NO Decomposition Catalyst Cu-ZSM-5

Dean C. Sayle,*,† C. Richard A. Catlow,† Julian D. Gale,‡ Marc A. Perrin,§ and Patrice Nortier§

Davy-Faraday Laboratory, The Royal Institution of Great Britain, 21 Albemarle Street, London W1X 4BS, United Kingdom, Department of Chemistry, Imperial College, South Kensington, London SW7 2AY, United Kingdom, and Centre de Recherche de Rhône-Poulenc, 52 Rue de la Haie Coq, 93308 Aubervilliers Cedex, France

Received: November 5, 1996; In Final Form: February 10, 1997[⊗]

Static atomistic simulation techniques have been employed to identify the low-energy configurations for copper ions within the Cu-ZSM-5 catalyst. We find that both isolated copper and copper clusters form within the zeolite channels, 80% of which are associated with framework aluminum species. A particularly stable and common species comprises two copper ions bridged with extra-framework OH species, which we propose may be a useful model for the active site in Cu-ZSM-5 catalysts.

Introduction

One of the major current concerns worldwide is the reduction of global air pollution, a component of which is NO_x gas, emitted, in part, from combustion engines. The discovery by Iwamoto and co-workers[1] that Cu-ZSM-5 zeolites catalyze the decomposition of NO at high conversion has fueled much interest in these systems,[2−8] in particular with respect to car-exhaust catalysis.[9] However, various factors preclude the Cu-ZSM-5 systems from commercial viability as exhaust catalysts; these include thermal instability, a narrow (and therefore inadequate) range of temperatures associated with optimal performance, the effects of catalyst poisons such as sulfur compounds, and the effects of engine operation leading to varying emissions of hydrocarbons and nitrogen oxides.[9] Moreover, since any combustion process is going to produce almost 16% water vapor, catalytic systems must be stable for long times in such wet environments.[4] Considerable efforts have therefore been focused on developing catalysts without these limitations. Such studies would be greatly assisted by improved knowledge of the structure of the active sites in the Cu-ZSM-5 system. In the present work, we therefore address the question of the structure and location of these sites using computer-simulation techniques.

Cu-ZSM-5 catalysts are prepared by ion exchange, starting from Na(ZSM-5). The most active systems, for the decomposition of NO, are overexchanged, where the Cu(I)/Al ratio exceeds 1.0. These copper species have been shown, using Cu^+ photoluminescence spectroscopy, to occupy extra-framework positions in the vicinity of framework Al.[10] However, as noted, the most active zeolites are those in which there are more than one copper species for each framework aluminum; the excess copper must therefore adopt additional locations within the zeolite. Moreover, the increase in catalytic performance with increasing copper loading (>1.0)[11] suggests that excess copper species enhance catalytic activity. Identification of these structures is clearly a key requirement in guiding the design of catalysts which address the deficiencies of the present material.

Various models[8,11−13] have been suggested for the configuration of the active site, and all agree that isolated Cu species together with copper pairs bridged by lattice oxygen or hydroxyl groups are present in the active catalyst. A detailed study by Grunert et al.[14] identified six distinct copper species with respect to environment, location, or degrees of aggregation. Furthermore, they suggested that both the isolated copper *and* the copper clusters are necessary to provide optimum catalytic performance.

In this study, we identify low-energy configurations for extra-framework copper using energy-minimization techniques. Such applications of computer-simulation techniques are well-known to provide valuable complementary information to experiment, and in the present case, they allow us to develop detailed models for the extra-framework copper clusters and their interactions with the host zeolite lattice.

Structure of ZSM-5

The idealized structure of silicalite, illustrated in Figure 1, comprises interconnecting straight (5.6×5.3 Å) and sinusoidal channels (5.1×5.5 Å) with orthorhombic space group symmetry *Pnma*, $a = 20.1$ Å, $b = 19.9$ Å, $c = 13.4$ Å[15−17] and contains 96 silicon and 192 oxygen atoms (SiO_2), resulting in a framework density of 17.9 T sites/1000 Å^3. The synthetic zeolite, ZSM-5, has the same framework structure as silicalite, with a proportion of the silicon sites occupied by Al^{3+}. Two phases of the purely siliceous zeolite, silicalite, are known: the first to be identified[15] was the orthorhombic phase which contains 12 independent T sites; the second, a low-temperature monoclinic phase (which is ascribed to a shift of neighboring (010) pentasil layers), contains 24 independent T sites.[17] Previous computer-modeling studies[18] showed that energy-minimization techniques using shell model potentials were able to reproduce the monoclinic structure accurately. The same minimization procedures and interatomic potentials are employed in the present study with additional parameters to describe the interactions involving copper ions. Further details are given in the next section.

Potential Models and Minimization Methods

As noted, we have used standard static lattice methods, the methodologies of which are given in more detail elsewhere[19,20,24] and will only be treated in outline here. The methods are based on the calculation and minimization of the lattice energy of the system using the GULP program.[21] By "system" we are referring to the zeolite framework and, in this case, additional extra-framework species added. During the minimization, the positions of the framework and extra-framework ions are varied until a minimum energy configuration is achieved. The interatomic potentials used to describe the interactions between

† The Royal Institution of Great Britain.
‡ Imperial College.
§ Centre de Recherche de Rhône-Poulenc.
⊗ Abstract published in *Advance ACS Abstracts,* April 1, 1997.

S1089-5639(96)03459-7 CCC: $14.00

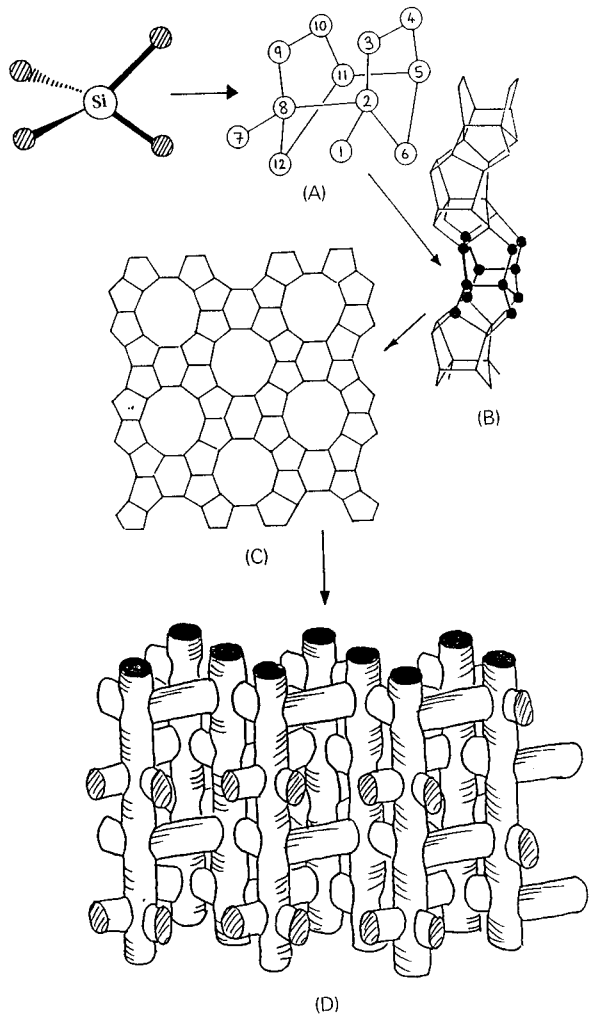

Figure 1. Diagrammatic representation of the ZSM-5 structure. (A) Secondary building blocks illustrating the 12 T sites which combine to form chain-type building blocks (pentasil layers (B)). These pentasil layers can combine to form the channel system of the ZSM-5 structure (C). A displacement of these pentasil layers along the (010) direction results in the monoclinic phase of the zeolite, and the subsequent reduction in symmetry allows for 24 independent T sites. (D) Schematic representation of the interconnecting channel system in the zeolite.

the component species of the system include long-range Coulombic terms and two- and three-body parameterized short-range repulsive potentials. Polarizability of the component species is introduced via the shell model.[22] The reliability of such calculations rests ultimately on the quality of interatomic potentials, and care must therefore be exercised in the choice of potential parameters. In this present study, the parameters for the zeolite are taken from the work of Jackson and Catlow,[23] which, as noted, reproduce accurately the monoclinic distortion observed at lower temperatures in silicalite.[18]

The short-range potential parameters for Cu(I)−O were obtained by fitting to the Cu_2O crystal structure and elastic constants using a *relaxed fitting* routine available within the GULP program. This powerful procedure enables fitting to the experimental crystal properties using residuals from the calculated properties obtained, at each step, from the *energy-minimised geometry* (and not the experimental geometry). This procedure is discussed and illustrated in more detail by Bush et al.[24] Attempts to derive a suitable potential for Cu(II)−O by fitting to the CuO structure proved unsuccessful. Indeed, it is most likely that it is not possible to represent CuO adequately within a two-body model. Instead, a potential for Cu(II)−O was taken from the study of Baetzold,[25] who was able to model

TABLE 1: (a) Short-Range Potential Parameters of the Form $E(r) = A\exp(-r/\rho) - Cr^{-6}$,[a] (b) Short-Range Potential Parameters of the Form $E(r) = D_e[1 - \exp(-\alpha(r - r_o))]^2$, (c) Three-Body Terms of the Form $E(\Theta) = {}^1/_2K(\Theta - \Theta_o)$, and (d) Ionic Charges and Shell Model Parameters

Section a

species	A, eV	ρ, Å	C, eV Å^6	cutoff, Å
$Si^{4+}-O^{2-}$	1283.91	0.321	10.66	20.0
$Si^{4+}-O^{1-}$	983.56	0.321	10.66	20.0
$Al^{3+}-O^{2-}$	1460.30	0.299	0.00	10.0
$Al^{3+}-O^{1-}$	1142.68	0.299	0.00	10.0
$O^{2-}-O^{2-}$	22764.00	0.149	27.88	20.0
$O^{2-}-O^{1-}$	22764.00	0.149	27.88	20.0
$O^{1-}-O^{1-}$	22764.00	0.149	27.88	20.0
$Cu^{2+}-O^{2-}$	712.80	0.327	0.00	10.0
$Cu^{2+}-O^{1-}$	546.20	0.327	0.00	10.0
$Cu^{+}-O^{2-}$	7000.00	0.209	0.00	10.0
$Cu^{+}-O^{1-}$	5035.00	0.209	0.00	10.0
$O^{2-}-H$	311.97	0.250	0.00	10.0

Section b

	D_e, eV	α, Å^{-1}	r_o, Å
$O^{1-}-H$	7.0525	2.1986	0.949

Section c

species	K, eV rad^{-2}	Θ_o, deg
$O^{2-}-Si^{4+}-O^{2-}$	2.097	109.47
$O^{2-}-Al^{3+}-O^{2-}$	2.097	109.47

Section d

species	charge, e	spring const, eV Å^{-2}
Si^{4+} core	4.0	rigid ion
O^{2-} shell	−2.869	74.92
O^{2-} core	0.869	
O^{1-} core	−1.426	rigid ion
H core	0.426	rigid ion
Cu^{2+} core	2.0	rigid ion
Cu^{+} core	1.0	rigid ion
Al^{3+} core	3.0	rigid ion

[a] Where the oxygen of the hydroxyl species is designated O^{1-}.

accurately the Cu(II)−O bond distances in the orthorhombic $YBa_2Cu_3O_7$ to within 0.02 Å. The potential parameters for the hydroxyl group were taken from the study of Schroder et al.,[26] who used the model to probe the siting of framework Al and bridging OH groups in H-ZSM-5. The charges assigned to the hydroxyl oxygen ion are fractional, and therefore, the short-range potentials must be consistent with the electrostatic interaction of the formally charged silicon and aluminum ions; to achieve that, the authors refitted the Al−O and Si−O short-range potentials, accommodating the reduction in charge by modification of the A parameter in the Buckingham (see Table 1a caption) short-range potentials. Accordingly, in this study, the Cu(I)−O short-range parameter (for the oxygen of the OH group) was refitted to the Cu_2O crystal structure assuming a partial charge (assigned to the oxygen ion in the OH) for the oxygen. As the Cu(II)−O potential was not fitted to CuO, this procedure cannot be repeated for Cu(II). Instead, the A parameter of Cu(II)−O for oxygen of the OH group was scaled by the ratio of the A parameters for the silicon−lattice oxygen $Si-O^{2-}$ (A_1) and to that of the silicon−hydroxyl oxygen $Si-O^{p}$ (A_2):

$$A[\mathrm{Cu(II)-O}] = A_1[\mathrm{Si-O^{2-}}]/A_2[\mathrm{Si-O^{p}}] \qquad (1)$$

where O^p represents oxygen with the partial charge of −1.426 employed in describing the OH groups. The potential parameters employed in this study are all given in Table 1.

TABLE 2: Bond Distances, Coordination Numbers (CN), and Association with Framework Al (if Applicable) for Each of the Copper Ions within Each of the 10 Systems, where Section a Is Representative of the Lowest Energy Structures, Section b the Next Lowest Energy, and So Forth[a]

	Cu−O, Å	Cu−OH, Å	Cu−Cu, Å	Cu−Al, Å	CN	type
			Section a			
Cu(II)	2.02, 2.14, 2.31	1.72	3.29	2.88	4	C1
Cu(I)	2.07, 2.09	1.91			3	
Cu(II)	2.05, 2.09, 2.14, 2.34	1.83			4	B8
Cu(II)	2.01, 2.28	1.84, 1.84	2.85	3.21	4	C2
Cu(II)	2.01, 2.13	1.86, 1.87		2.93	4	
Cu(I)	2.01, 2.02, 2.10	2.16		2.76	4	A11
Cu(I)	2.02, 2.07, 2.10, 2.28			2.80	4	A14
Cu(I)	2.00, 2.01			2.76	2	A6
			Section b			
Cu(II)		1.62, 1.77	3.35		2	C3
Cu(I)	2.08, 2.08	1.91			3	
Cu(II)	2.03, 2.08	1.83, 1.84	2.82	2.91	4	C2
Cu(II)	2.03, 2.06	1.86, 1.86		2.90	4	
Cu(II)	1.93, 1.94, 2.04, 2.19			2.91, 3.14	4	A12
Cu(I)	1.97, 1.98			2.71	2	A6
Cu(I)	2.00, 2.11, 2.13, 2.15, 2.19			2.62, 2.90	5	A5
Cu(I)	2.07, 2.07, 2.14, 2.14, 2.28			2.58	5	A9
			Section c			
Cu(II)	1.82, 2.23	1.70	3.40	2.83, 3.35	3	C1
Cu(I)	2.19	1.99, 2.02			3	
Cu(II)	1.82, 1.83			2.76	2	A6
Cu(II)	2.03, 2.05	1.63		2.93	3	B2
Cu(II)	1.96, 2.02, 2.18	1.69	3.06	2.87	4	C1
Cu(I)	1.96, 2.09	1.89		2.76	3	
Cu(I)	2.02, 2.14, 2.18, 2.23			2.87	4	A8
Cu(I)	1.98, 2.05, 2.07, 2.15			2.69, 3.21, 3.22	4	A4
			Section d			
Cu(II)	1.97	1.72, 1.79	3.32		3	C3
Cu(I)	2.09, 2.14	1.92			3	
Cu(II)	1.98, 2.00	1.69	3.26	2.87	3	C1
Cu(I)	2.07, 2.11	1.91			3	
Cu(II)	1.92, 1.92, 1.97			2.70, 2.71	3	A7
Cu(II)	2.11, 2.17, 2.18	1.74	3.40	3.38, 3.39, 3.39	4	C1
Cu(I)	1.94, 2.28	1.95		2.88	3	
Cu(I)	2.08, 2.16, 2.20, 2.22			2.72	4	A11
			Section e			
Cu(II)	1.96, 1.97	1.66	3.44	2.85	3	C3
Cu(II)	2.06, 2.14	1.74, 1.83		2.88	4	
Cu(II)	1.94, 2.08	1.67	3.04	2.83	3	C1
Cu(I)	2.01, 2.05	1.95		2.77, 3.31	3	
Cu(II)	2.08, 2.11	1.60		2.91	3	B2
Cu(I)	1.99, 2.02, 2.03			2.64, 2.95	3	A13
Cu(I)	1.99, 2.01, 2.14, 2.25			3.07, 3.23	4	A4
Cu(I)	1.99, 2.00, 2.09, 2.16			2.65, 3.00	4	A4
			Section f			
Cu(II)	1.90, 1.93, 2.09			2.81, 2.85	3	A7
Cu(II)	1.94, 2.05, 2.06			2.89	3	A7
Cu(II)	2.09, 2.13, 2.29	1.68	3.22	3.30	4	C1
Cu(I)	2.03, 2.09	1.93		3.02	3	
Cu(II)	2.02, 2.08	1.83		3.04	3	B6
Cu(I)	2.06, 2.20, 2.26, 2.30	2.13		2.58, 3.16	5	B7
Cu(I)	1.99, 2.00			2.73	2	A2
Cu(I)	1.98, 2.12, 2.13			2.71	3	A3
			Section g			
Cu(II)	1.87, 1.88, 2.11, 2.13			2.73, 2.81	4	A14
Cu(II)	1.98, 2.11, 2.20, 2.28			2.95	4	A8
Cu(II)	1.94, 2.01	1.67	3.04	2.83	3	C1
Cu(I)	2.02, 2.08, 2.17	1.93		2.67	4	
Cu(II)	2.04, 2.08, 2.22	1.83		2.91	4	B6
Cu(I)	2.01, 2.08, 2.14, 2.22			2.59, 3.34	4	A8
Cu(I)	2.05, 2.07, 2.07, 2.15	2.01			5	B8
Cu(I)	2.01, 2.04, 2.09			2.72	3	A3
			Section h			
Cu(II)	2.10, 2.22, 2.23	1.78	3.26		4	C4
Cu(II)	2.24	1.60, 1.88			3	
Cu(I)	1.97, 2.22, 2.27	2.08		3.01	4	
Cu(II)	1.99, 2.04	1.60		2.88	3	B2
Cu(II)	1.90, 1.95, 1.96			2.73, 2.78	3	A7
Cu(I)	2.03, 2.06, 2.16, 2.19, 2.23			2.67, 2.79	5	A5
Cu(I)	2.06, 2.16, 2.18, 2.26, 2.27			2.64, 3.23	5	A5
Cu(I)	2.01, 2.14, 2.26			2.78	3	A7

TABLE 2 (Continued)

	Cu−O, Å	Cu−OH, Å	Cu−Cu, Å	Cu−Al, Å	CN	type
			Section i			
Cu(II)	1.92	1.73			2	B1
Cu(II)	1.88, 1.88, 2.07, 2.29			2.79, 3.14	4	A4
Cu(II)	2.06, 2.11, 2.19	1.62			4	B3
Cu(II)	1.93, 1.98	1.69	3.11	2.83	3	C1
Cu(I)	2.00, 2.02	1.95		3.11	3	
Cu(I)	1.95, 1.97			2.74	2	A6
Cu(I)	2.07, 2.08, 2.14, 2.20				4	A11
Cu(I)	2.02, 2.07, 2.09			2.76	3	A10
			Section j			
Cu(II)	2.09, 2.10, 2.13, 2.15, 2.30				5	A5
Cu(II)	2.06, 2.11	1.60		3.02	3	B2
Cu(II)	2.09, 2.12, 2.17, 2.19	1.75		2.92, 3.33	5	B9
Cu(II)	1.93, 2.11	1.60		2.95	3	B2
Cu(I)	2.07, 2.10, 2.19, 2.24	2.03	3.79	2.90	5	C1
Cu(I)	2.09, 2.32	1.93			3	
Cu(I)	2.00, 2.01, 2.18, 2.28			2.73, 2.83	4	A8
Cu(I)	1.95, 2.01, 2.03			2.78, 3.16	3	A3

[a] The cluster types, in the final column, are illustrated in Figure 2.

Simulation Methodology

Our aim is to identify the low-energy configurations of copper within the ZSM-5 zeolite. We consider models appropriate to the active Cu-ZSM-5 system; in particular, we have chosen one with a high Si/Al ratio to reduce the computational expense of examining dilute systems. The system considered is taken from Iwamoto et al.,[27] which comprises 7.6 aluminum atoms per unit cell (which contains 96 T sites) and 157% copper loading where the exchange level is calculated as 2 (amount of Cu(II))/(amount of Al). Assuming equal loading of Cu(I) and Cu(II),[11] this corresponds to approximately 4Cu(I) and 4Cu(II) per 96 silicon T sites with charge neutrality facilitated via the addition of 4 OH^- species. Trial structures for this system were constructed by replacing, at random, 8 of the 96 T sites with aluminum ions. The 4Cu(II), 4Cu(I), and 4OH^- extra-framework species are introduced, again randomly, with the only constraint imposed being a simple proximity criterion to prevent excessive steric overlap; potentially overlapping extra-framework species are rejected, and a further random insertion is applied. Two thousand "trial structures" were obtained, and the energy of each system is calculated. Full energy minimization was then applied to the 20 systems with the lowest unrelaxed energy.

Initially, minimization is applied only to the extra-framework species, as the ZSM-5 framework is already close to its equilibrium position. (Aluminum substituted at silicon sites is expected to make only minor perturbations to the zeolite framework structure compared with the relaxation expected for the extra-framework species.) Applying minimization only to these extra-framework species, which are expected to be far from the energy minimum positions, substantially reduces the computational expense: specifically, we need only consider 16 atoms (extra-framework copper and OH) compared with 512 atoms (which includes the zeolite framework). Following the initial minimization with respect to the extra-framework species, a full energy minimization, in which the zeolite framework also relaxes, is performed.

All of the configurations were initially optimized with a maximum short-range potential cutoff of 12 Å. By adjusting the Ewald summation parameter to decrease the real space cutoff at the expense of the reciprocal space series, it was possible to achieve an increase in speed of almost a factor of 3.

The most efficient minimization procedure was found to be to use a BFGS[28] update of the Hessian starting initially from a unit matrix, followed by rational functional optimization once the gradient norm becomes small. The use of the exact second derivative matrix during the initial minimization is more expensive and is only slightly more beneficial when the systems are distant from the minimum. As the atoms approach the minimum, it was found that there are a significant number of imaginary modes in the Hessian due to motions, such as rotation of hydroxyl groups. The use of rational function optimization rapidly removes these modes and ensures that a genuine minimum is attained.

In summary, our approach is to place randomly framework Al and extra-framework Cu(II), Cu(I), and OH^- species into the zeolite with loadings equivalent to the experimentally observed overexchanged and catalytically active Cu-ZSM-5 system. Energy-minimization techniques are then applied only to the most stable 20 (out of 2000) configurations generated. This approach therefore allows for a high number of initial configurations to be considered, and consequently, no constraints need be imposed on the location of the added species (apart from steric considerations) which may artificially influence any final configuration. Furthermore, because the clusters are not constructed explicitly—rather the minimization procedure directs the extra-framework species to aggregate—the number of extra-framework species in each cluster may vary.

The relative ordering by energy of the most stable 20 configurations initially generated is not likely to be reproduced after a full energy minimization. Indeed, the most stable system before minimization was not the most stable after minimization. However, it was found that those systems, less favorable energetically before minimization, were likely to result in energetically unfavorable final configurations. Moreover, it is unlikely that our procedure has failed to identify any of the significant low-energy structures.

Results and Discussion

Out of 20 systems considered for full energy minimization, 15 systems successfully converged, taking on average 1000 cycles to converge (about 100 h on a Silicon Graphics power challenge). The 10 systems with the lowest energy were then examined in detail with respect to the configuration and location of the various copper species within the ZSM-5 host lattice. Table 2 explicitly describes the configurations of each of the copper species in the 10 systems considered. To aid interpretation of the copper clusters, the final column of Table 2 gives the cluster type (Figure 2) which have been categorized as types A, B, and C according to the complexity of the cluster: type A comprises isolated copper species, type B comprises an isolated copper species and extra-lattice OH^-, and type C comprises aggregated copper clusters. For example, if we consider the lowest energy system (Table 2a), six clusters were observed, two of which contain copper pairs. The first cluster contains

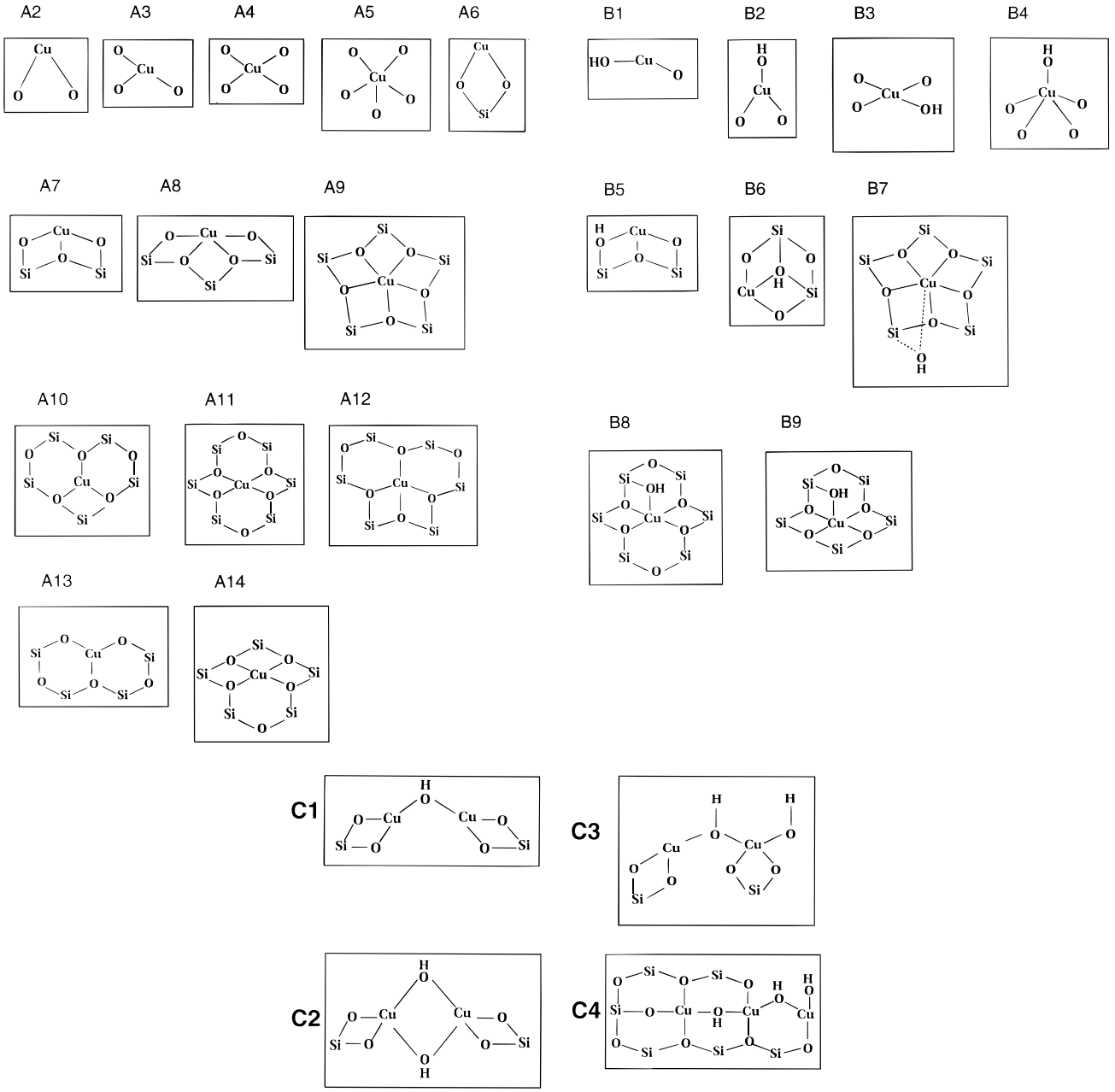

Figure 2. Representation of the various cluster types identified for the copper species in the ZSM-5 zeolite: type A, type B, or type C according to the complexity of the cluster, where type A comprises isolated copper species, type B isolated copper species and extra-lattice OH^-, and type C aggregated copper clusters. We note that for reasons of clarity, the first shell of oxygens around the copper species may not all be displayed for cluster types C1−C4.

Cu(II) and Cu(I) adopting a configuration represented by cluster type C1 (Figure 2). Cu(II) is coordinated to four oxygen ions, one of which is the OH^- species. Cu(II) is also associated with a lattice Al species (2.88 Å), and the Cu(II)−Cu(I) distance is 3.29 Å.

The calculations reveal that 41% of all the copper species introduced into the ZSM-5 are paired. Association with framework aluminum species plays an important role in stabilizing these systems, which is reflected in the fact that 80% of all the copper species are associated with one or more framework aluminum species. Experimentally, Wichterlova et al.[12] have observed copper species associated with framework aluminum using Cu^+ luminescence techniques.

The average Cu−O bond distances (Table 3) are calculated to be 1.96 Å (Cu(II)−O) and 2.07 Å (Cu(I)−O), compared with 1.96 Å observed experimentally.[14] In light of the diversity and complexity of the various configurations of the copper species within the ZSM-5 zeolite, these results show good agreement with the experimental observations. We also note that the average coordination number for the Cu(I) species is 0.15 higher than that of Cu(II).

TABLE 3: Coordination Numbers (CN) and Cu−O Bond Distances Averaged over All 10 Systems for the Cu(II) and Cu(I) Species

	CN	O, Å	OH, Å	Cu−O av, Å
Cu(II)	3.375	2.05	1.76	1.96
Cu(I)	3.525	2.09	1.95	2.07

Figure 3 illustrates the occupancy of associated copper species, while Figure 4 gives the occupancy for isolated copper species together with their coordination numbers. It is expected that the higher the occupancy, the greater the stability of the particular configuration. Clearly we observe a preponderance of C1-type clusters. Indeed, 25% of **all** the copper species in each of the 10 systems considered have this type of configuration. On closer inspection, 9 of the 10 C1-type clusters were

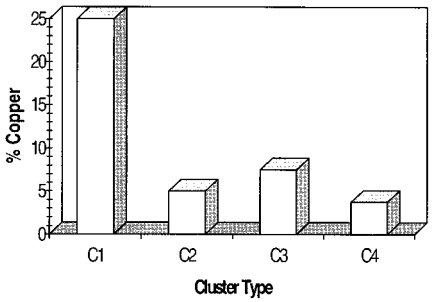

Figure 3. Occupation levels of the copper pairs over all 10 systems considered.

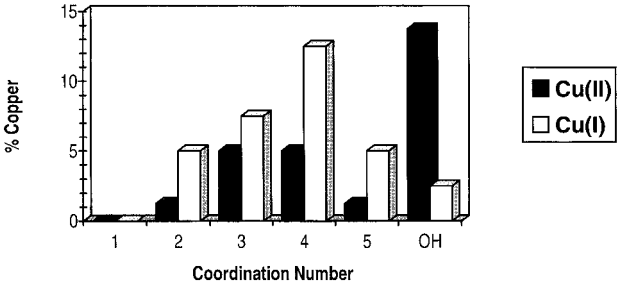

Figure 4. Occupation levels of the isolated copper species over all 10 systems considered. The copper species are grouped according to their coordination number within the host ZSM-5 lattice or whether the copper is associated with a hydroxyl group.

of mixed valence [Cu(II)−OH−Cu(I)] and the other, isovalent copper, Cu(I)−OH−Cu(I). We note that the latter cluster was observed in the system with the lowest energy, and furthermore, as the Cu−Cu distance is 3.79 Å, we suggest the association is weak. The very high proportion of mixed valent copper pairs [Cu(II)−OH−Cu(I)] suggests these species are more stable than alternative configurations within the ZSM-5 host lattice and as such represent a likely model for the active site within Cu-ZSM-5 based catalysts.

Only one cluster contained three copper ions (with one of the copper species located within a "cage" of the ZSM-5), and no clusters contained four or more copper species. This result is somewhat surprising since the formation of "tricopper clusters" could be readily achieved by the addition of "HO−Cu" to an existing copper pair; yet with only one example generated by our procedure, we might tentatively suggest that the ZSM-5 host lattice does not stabilize the formation of higher order copper species within its channel system.

Figure 5 illustrates the configuration and location of all the copper species in the lowest energy system (Table 2a), while Figures 6 and 7 illustrate, with more clarity, the configurations of single copper species and copper pairs, respectively, in this lowest energy system. The proposed model for the active site [Cu(II)−OH−Cu(I)] is illustrated to the left of Figure 7. We note the cluster is anchored to the zeolite wall via a framework aluminum species. This configuration suggests a "cluster" charge of +1, which indicates instability. However, the figure depicts only the *local* structure; any charge-compensating hydroxyl or framework aluminum will be present within the full primitive cell which comprises 4Cu(II), 4Cu(I), 4OH, and $8Al^{3+}$.

It is desirable to extend our calculations to investigate the reaction mechanism of the Cu-ZSM-5 catalyst. In future studies, we will therefore employ a quantum mechanical description of our proposed model for the active site, identified in this present study.

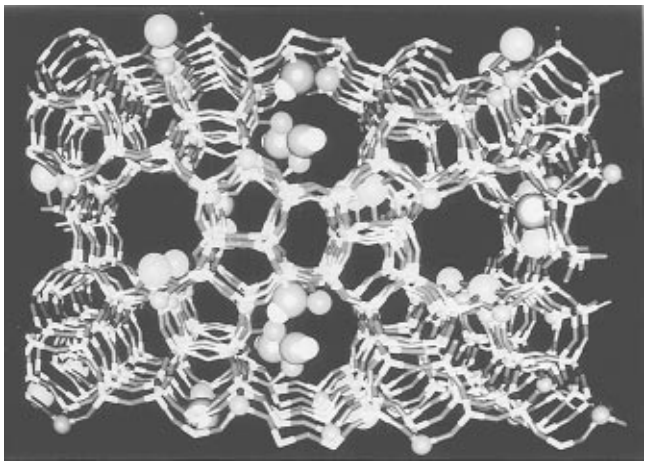

Figure 5. Illustration of the configurations of the copper species in the lowest energy system (Table 2a). Silicon are represented by light sticks and lattice oxygen by darker sticks, Cu(II) and Cu(I) species are represented by small and large balls, respectively, and hydroxyl groups are the connected small and large balls where hydrogen is the smaller lighter ball of the two.

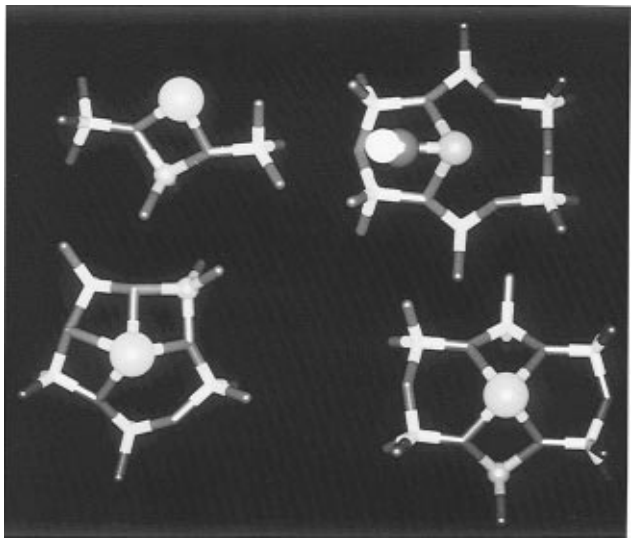

Figure 6. Illustration of the single copper species within the ZSM-5 host lattice. Notation is as in Figure 5.

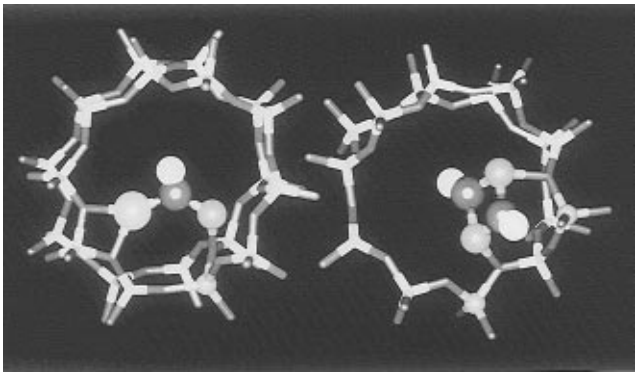

Figure 7. Illustration of copper pairs within the ZSM-5 host lattice. Notation is as in Figure 5.

Conclusion

Using energy-minimization techniques, we have developed models for the structure of copper-containing clusters in overexchanged Cu-ZSM-5 catalysts. In particular, we suggest that the most likely candidates for the active sites in these systems comprise copper pairs bridged via OH groups. It is probable that these clusters are anchored via one or more

framework aluminum species, and we suggest they contain mixed rather than isovalent copper species.

Acknowledgment. We thank R. P. for financial support. Our thanks go to Professor R. W. Joyner and Dr. G. Sankar for many useful discussions. We also acknowledge MSI for the provision of the InsightII software of their catalysis and sorption project.

References and Notes

(1) Iwamoto, M.; Yokoo, S.; Saskai, S.; Kagawa, S. *J. Chem. Soc., Faraday Trans. 1* **1981**, *77*, 1629.
(2) Shelef, M. *Catal. Lett.* **1992**, *15*, 305 and references cited therein.
(3) Schoonheydt, R. A. *Catal. Rev.-Sci. Eng.* **1993**, *35*, 129.
(4) Burch, R., Ed. *Catal. Today* **1995**, *26*, 97.
(5) Ansell, G. P.; Diwell, A. F.; Golunski, S. E.; Hayes, J. W.; Rajaram, R. R.; Truex, T. J.; Walker, A. P. *Appl. Catal. B: Environ.* **1993**, *2*, 81.
(6) Hall, W. K.; Valyon, J. *Catal. Lett.* **1992**, *15*, 311.
(7) Spoto, G.; Bordiga, S.; Scarano, D.; Zecchina, A. *Catal. Lett.* **1992**, *13*, 39.
(8) Moretti, G. *Catal. Lett.* **1994**, *28*, 143.
(9) Truex, T. J.; Searles, R. A.; Sun, D. C. *Platinum Met. Rev.* **1992**, *36*, 2.
(10) Dedecek, J.; Wichterlova, B. *J. Phys. Chem.* **1994**, *98*, 5721.
(11) Iwamoto, M.; Yahiro, H.; Tanda, K.; Mizuno, N.; Mine, Y.; Kagawa, S. *J. Phys. Chem.* **1991**, *95*, 3727.
(12) Wichterlova, B.; Dedecek, J.; Vondrova, A. *J. Phys. Chem.* **1995**, *99*, 1065.
(13) Hamada, H.; Matsubayshi, N.; Shimada, H.; Kintaichi, Y.; Ito, T.; Nishijima, A. *Catal. Lett.* **1990**, *5*, 189.
(14) Grunert, W.; Hayes, N. W.; Joyner, R. W.; Shpiro, E. F.; Rafiq, M. R.; Siddiqui, H.; Baeva, G. N. *J. Phys. Chem.* **1994**, *98*, 10832.
(15) Flanigen, E. M.; Bennett, J. M.; Grose, R. W.; Cohen, J. P.; Patton, R. L.; Kirchner, R. M.; Smith, J. V. *Nature* **1978**, *271*, 512.
(16) Olson, D. H.; Kokotailo, G. T.; Lawton, S. L.; Meier, W. M. *J. Phys. Chem.* **1981**, *85*, 2238.
(17) van Koningsveld, H.; Jansen, J. C.; van Bekkum, H. *Zeolites* **1990**, *10*, 235.
(18) Bell, R. G.; Jackson, R. A.; Catlow, C. R. A. *J. Chem. Soc., Chem. Commun.* **1990**, 782.
(19) Catlow, C. R. A.; Mackrodt, W. C., Eds. *Computer Simulation of Solids*; Lecture Notes in Physics 166; Springer: Berlin, 1982.
(20) Catlow, C. R. A., Ed. *Modelling of Structure and Reactivity in Zeolites*; Academic: London, 1992.
(21) Gale, J. D. *J. Chem. Soc., Faraday Trans.* **1997**, *93*, 629.
(22) Dick, B. G.; Overhauser, A. W. *Phys. Rev.* **1958**, *112*, 90.
(23) Jackson, R. A.; Catlow, C. R. A. *Mol. Simul.* **1988**, *1*, 207.
(24) Bush, T. S.; Gale, J. D.; Catlow, C. R. A.; Battle, P. D. *J. Mater. Chem.* **1994**, *4*, 831.
(25) Baetzold, R. C. *J. Am. Ceram. Soc.* **1990**, *73*, 3185.
(26) Schroder, K.-P.; Sauer, J.; Leslie, M.; Catlow, C. R. A. *Zeolites* **1992**, *12*, 20.
(27) Iwamoto, M.; Yahiro, H.; Mizuno, N.; Zhang, W.-X.; Mine, Y.; Furukawa, H.; Kagawa, S. *J. Phys. Chem.* **1992**, *96*, 9360.
(28) Press, W. H.; Teukolsky, S. A.; Vetterling, W. T.; Flannery, B. P. *Numerical Recipes*, 2nd ed.; Cambridge University: Cambridge, 1992.